

## Probing the Effect of Water–Water Interactions on Enzyme Activity with Salt Gradients: A Case-Study Using Ribonuclease t1

David L. Beauchamp and Mazdak Khajepour\*

Department of Chemistry, University of Manitoba, Winnipeg MB R3T 2N2, Canada

Received: August 10, 2010; Revised Manuscript Received: October 27, 2010

Water molecules interact with one another via hydrogen bonds. Experimental and theoretical evidence indicates that these hydrogen bonds occur in two modalities—high- and low-angle hydrogen bonding—and that the addition of various solutes to water affects only the number of water molecules participating in a specific type of hydrogen bond interactions, not the nature of the water–water interactions. In this work, we have investigated the effect of each of these hydrogen bonding types upon the activity of the enzyme ribonuclease t1. This was done through perturbation of the water hydrogen bonding distribution by using various salts. Our results indicate that various salts differ in their ability to reduce the enzymatic activity of ribonuclease t1, and this ability is well correlated with the ability of each salt to promote high-angle hydrogen bonding in water. By applying the two-phase model of liquid water (i.e., liquid water being modeled as an equilibrium existing between two phases, LD and HD water), we demonstrate that our results are compatible with the assumption that increasing the population of high-angle hydrogen bonds among water molecules stabilizes the more compact, less active conformations of the enzyme. This indicates that the structures that proteins adopt in water solution depend upon the nature of interactions between water molecules.

The field of enzymology has progressed considerably since the original experiments of Michaelis and Menten.<sup>1</sup> Following Koshland's paper on the induced fit mechanism of enzyme catalysis,<sup>2</sup> a large body of important work has led to the clarification of many fundamental issues in enzyme chemistry. These issues include understanding how enzymes stabilize the transition state of the reaction that they catalyze,<sup>3–5</sup> what the relationship is between the macromolecular structure of enzymes and their reactivity,<sup>6</sup> and how the enzyme molecules undergo dynamic conformational changes as they move through the catalytic cycle.<sup>7–9</sup> In all of the work cited above, the focus has been upon the enzyme molecule itself; however, enzymes also require hydration in order to be active,<sup>10</sup> underlining the important role that water plays in enzyme activity. In fact, recent work<sup>11–16</sup> has caused a major revision in our understanding of the role that water molecules play in protein structure and function. We now know that the aqueous solvent is not inert but rather is an active participant in protein structure and dynamics; for example, the cause of many protein structural fluctuations in solution has been suggested to be the dielectric fluctuations of solvent water molecules.<sup>17</sup> Therefore, a complete understanding of the enzyme mechanism also requires a clear understanding of how water molecules interact with one another and how these interactions lead to the stabilization of different conformations of the enzyme.

It has long been known that water molecules interact with each other via hydrogen bonds.<sup>18</sup> Theoretical calculations<sup>19</sup> performed to determine the population distribution of the water–water hydrogen bond angles in liquid water suggest that the hydrogen bonds exhibit a bimodal population distribution with constant peak and saddle positions. These calculations confirm that water molecules can interact with each other in two modalities, forming low- or high-angle hydrogen bonds with

one another. Other calculations<sup>20</sup> have demonstrated that the addition of various solutes to aqueous solutions changes the populations of the distribution peaks but not their locations, indicating that solutes affect the number of water molecules participating in a specific hydrogen bonding interaction, not the nature of water–water interactions. This bimodal distribution of hydrogen bonding interactions in water is consistent with the various two-state models used to describe liquid water.<sup>21–26</sup> In these models, liquid water is assumed to be a mixture of two states at equilibrium with one another: one state has the water molecules participating in high-angle water–water hydrogen bonds similar to those present in ordinary ice (highly ordered low-density water, water<sub>LD</sub>), and the other state has the water molecules participating in low-angle (bent) hydrogen bonds (high-density water, water<sub>HD</sub>). These two-state descriptions of water are extremely useful because they provide a macroscopic thermodynamic framework in which to quantify the effects of temperature,<sup>27,28</sup> pressure,<sup>28</sup> and various solutes<sup>29,30</sup> upon the population distribution of the hydrogen bonding interactions in water. This allows researchers to investigate the different roles that low- and high-angle hydrogen bonding interactions in water play in the stabilization of biomolecules.

The hydration of biomolecules such as proteins is a complex process because they are composed of charged, polar, and hydrophobic amino acid residues. When proteins are dissolved in water, these three types of residues interact with water molecules in their vicinity to form a layer of interfacial water, which is the protein hydration layer. Various studies performed on protein stability indicate that the hydration layer greatly contributes to protein stability.<sup>31,32</sup> The protein hydration layer is formed from a dynamic network of water molecules<sup>33</sup> connected via hydrogen bonds that interact with each other and the protein molecule with a large degree of cooperativity.<sup>34,35</sup> Interactions between different segments of the protein and with water will cause the hydrogen bonding properties of the water in the hydration layer to be different from those in pure water;

\* To whom correspondence should be addressed. E-mail: khajepo@cc.umanitoba.ca. Tel: 204-272-1546.

in other words, they will shift the equilibrium between water<sub>LD</sub> and water<sub>HD</sub>. In fact, it has been shown that transitions between the native and molten globule states of proteins are accompanied by changes in the hydrogen bond network of the hydration layer, demonstrating the intimate relationship between hydration dynamics with protein fluctuations and their folding structures.<sup>34</sup> To understand this intimate relationship, it is essential to determine how changing the population distribution of water–water hydrogen bonding interactions affects the stability of particular protein conformations.

An important method for studying the role that water–water interactions play in protein stability is perturbing the protein–water system by adding a third component in a significant concentration.<sup>33,36–40</sup> In this work, the third component is a salt species. It has long been known that the solvation of salts in water perturbs the hydrogen bonding network of water molecules, causing changes in the water structure.<sup>41–44</sup> Experimentally, these changes are often observed in highly concentrated saline solutions, which may raise some questions about the relevance of these results to biological systems. However, the protein hydration layer presents a special case: proteins have charged residues on their surface, and ions of opposite charge interact favorably with these residues, leading to the migration of these species to the solvation shell<sup>45</sup> and enriching the local concentration of ions in the vicinity of the protein relative to that of the bulk. Therefore, the addition of ionic species to aqueous solutions of proteins will perturb the hydrogen bonding network of the protein hydration layer much earlier than that of the bulk water molecules. This causes the hydrogen bonding network of the protein hydration layer to be very sensitive to changes in salt concentration in the bulk solution, which can result in significant changes in the thermodynamic properties of biomolecules as salt is added.

In this work, we have probed the role of water–water hydrogen bonding with respect to the catalytic properties and, by extension, the structure of the model enzyme ribonuclease t1 (RNase t1). The RNase t1 enzyme is an ideal model system because it is a very well studied enzyme with well-defined catalytic, structural, and dynamic properties; it is a very thermodynamically stable enzyme; and it has a lone tryptophan residue (W59) that can be utilized as a straightforward probe of protein structure. The protein hydration layer was probed by perturbing the protein–water system by adding various alkali chloride salts to the protein solution. Chloride salts were chosen because the anion does not bind to the protein.<sup>46</sup> The enzyme-catalyzed hydrolysis of guanylyl-3′ → 5′-cytidine (GpC) was the reaction used to measure enzyme activity.<sup>47,48</sup> This activity was characterized by the enzyme specificity constant  $k_{\text{cat}}/K_{\text{m}}$ , a parameter that is sensitive to both enzyme affinity and catalytic ability. We demonstrate that the addition of salts causes the enzyme to lose its activity reversibly and adopt a more compact conformation. We have observed that the salts differ in their efficacy to inactivate RNase t1 and that their inactivation efficacy depends upon their ability to promote linear hydrogen bonding, thereby increasing the amount of water<sub>LD</sub>. This work demonstrates that increasing the population of linear hydrogen bonds promotes a more compact, less flexible form of the enzyme and for the first time establishes a direct correlation between water–water interactions and enzyme activity.

## Materials and Methods

**Materials.** Ribonuclease t1 (RNase t1) solution in 2.8 M ammonium sulfate was purchased from Worthington Biochemical Corporation (Lakewood, NJ). Guanylyl-5′-mono-

phosphate (5′-GMP), guanylyl-3′ → 5′-cytidine (GpC), and acrylamide and *N*-acetyl-L-tryptophanamide (NATA) were purchased from Sigma (St. Louis, MO). All experiments were done in pH 5.5 bis-tris buffer from Sigma (St. Louis, MO). All of the salts used were purchased from Fisher Scientific (Fair Lawn, NJ).

**Methods. Dialysis.** To eliminate the effect of ammonium sulfate in the RNase t1 storage solution, the enzyme was dialyzed prior to use for kinetic and fluorimetric assays. RNase t1 was placed in 1 L of a dialysis buffer (10 mM bis-tris, 10 mM NaCl at pH 5.5) for 1 h at 4 °C. This was repeated twice more in fresh buffer each time for a total of 3 h of dialysis in 3 L of dialysis buffer. The dialysis tape (MWCO = 6000–8000) used was purchased from Spectrum Laboratories, Inc. (Rancho Dominguez, CA). Dialysis had no deleterious effect on enzyme activity.

**UV–Vis Spectroscopy.** Kinetic measurements were performed using a Thermo Scientific Helios Zeta UV–vis spectrophotometer (Dubuque, IA) in a 10 × 10 mm<sup>2</sup> quartz cuvette. We determined the kinetic parameter  $k_{\text{cat}}/K_{\text{m}}$  (the specificity constant) using the methodology of Walz and co-workers.<sup>48</sup> Specifically, kinetic traces were obtained by adding RNase t1 to a 10 μM solution of GpC at pH 5.5 and monitoring the absorbance at 280 nm (where the final concentration of RNase t1 is 2.9 nM). The enzyme hydrolyzes the dinucleotide, causing an increase in absorbance at 280 nm. Because the amount of GpC is less than 1/20 of the  $K_{\text{m}}$  value (220 μM),<sup>47</sup> the Michaelis–Menten equation is reduced to pseudo-first-order form. The kinetic time traces (absorbance *A* vs time *t*) can be fitted to a monoexponential function in the form of (eq 1)

$$A = A_0 + B(1 - e^{-kt}); k = \frac{[E]k_{\text{cat}}}{K_{\text{m}}} \quad (1)$$

where [E] is the total concentration of enzyme,  $k_{\text{cat}}$  and  $K_{\text{m}}$  are the Michaelis–Menten parameters, and  $A_0$  and  $B$  are fitting constants. The kinetic data were analyzed using Sigma Plot (Point Richmond, CA) software. The reaction was thermostatically controlled at 25 °C with a Jeio-Tech refrigerating bath circulator (Des Plaines, IL).

**Fluorescence Spectroscopy.** Steady-state fluorescence spectra were measured on a Fluorolog-3 Horiba Jobin Yvon spectrofluorometer (Edison, NJ). The sample was held in a 10 × 10 mm<sup>2</sup> quartz cuvette equipped with a continuous stirrer. The data were analyzed with Sigma Plot (Point Richmond, CA) software. The reaction was thermostatically controlled at 25 °C with a Jeio-Tech refrigerating bath circulator (Des Plaines, IL). The 5′-GMP ligand has significant absorbance at high concentrations;<sup>49</sup> therefore, all fluorescence spectra reported have been corrected for inner filter effects.<sup>50</sup>

## Results

The activity of RNase t1 was determined by measuring the enzyme-catalyzed hydrolysis of GpC. Figure 1 depicts a typical kinetic trace obtained by adding RNase t1 to a 10 μM solution of GpC at pH 5.5 and monitoring the absorbance at 280 nm, where fitting the data to eq 1 yields  $k_{\text{cat}}/K_{\text{m}}$ . Salt effects on enzyme activity have been characterized by determining how  $k_{\text{cat}}/K_{\text{m}}$  varies with salt concentration. These results are shown in Figure 2 and depict the effects of various salts upon enzyme activity. The data show that the salt concentration causes a sizable decrease (more than 75%) in  $k_{\text{cat}}/K_{\text{m}}$  values. The addition of salt in the range of concentrations depicted in Figure 2 does

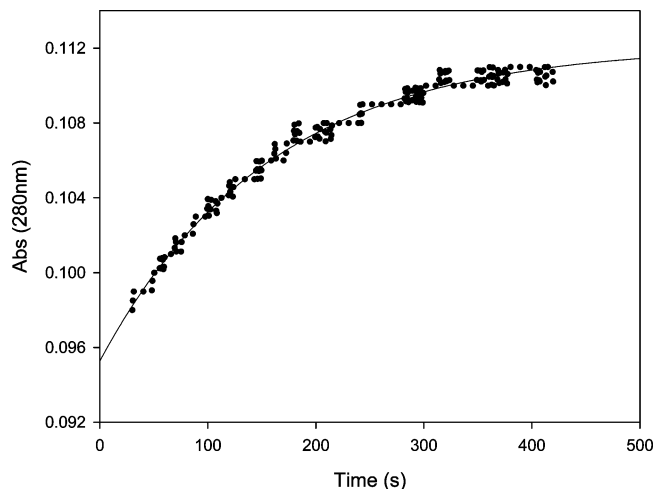


**Figure 1.** Typical kinetic trace obtained by adding RNase t1 to a 10  $\mu$ M solution of GpC at pH 5.5 10 mM bis-tris buffer. The absorbance is monitored at 280 nm.

not cause a significant decrease in the fluorescence of a 0.5  $\mu$ M solution of RNase t1, demonstrating that the decrease in activity is not due to enzyme precipitation. Furthermore, when RNase t1 solutions in high salt concentrations are diluted, the enzyme recovers its full activity, indicating that the loss of activity is a reversible process. It is also noteworthy that our values of  $k_{\text{cat}}/K_m$  at low salt concentrations correspond to those described in the literature.<sup>47,48</sup>

The binding of substrate-mimicking ligands to RNase t1 has been studied via fluorescence. Figure 3a,c depicts the steady-state fluorescence spectra of RNase t1 obtained by exciting the protein at 265 and 290 nm. These spectra differ significantly from one another because the spectrum in Figure 3c is obtained by selectively exciting the lone tryptophan residue (W59) of the protein. In contrast, the spectrum in Figure 3a has contributions from both tyrosine emission and tryptophan emission, with the tryptophan emission being caused by fluorescence resonance energy transfer (FRET) between the excited tyrosine residues and W59.<sup>50</sup> The data in Figure 3 show how the fluorescence

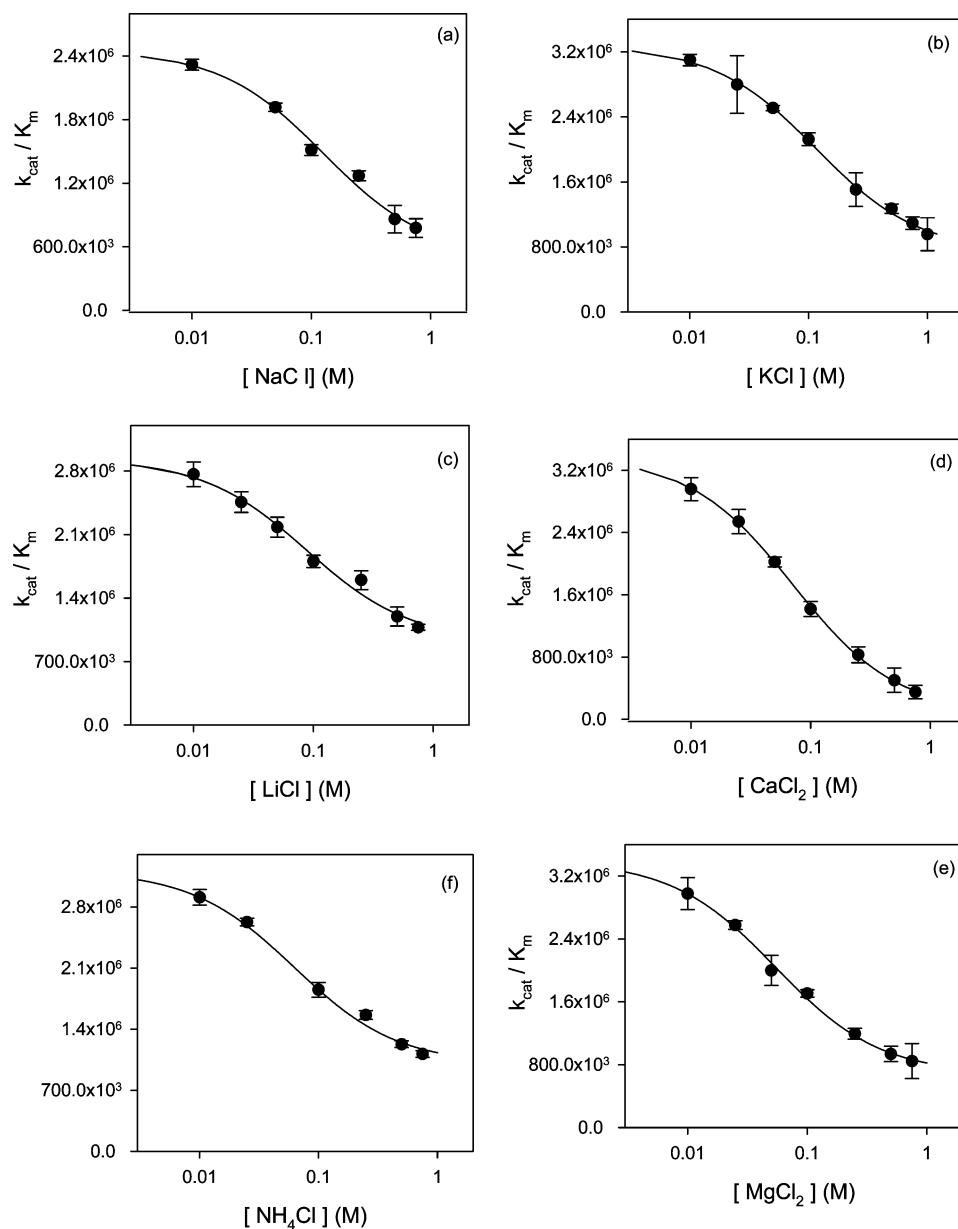


**Figure 2.** Effect of various salts upon the  $k_{\text{cat}}/K_m$  parameter of RNase t1 obtained from the enzyme-catalyzed hydrolysis of GpC. The solid lines are obtained by fitting the data to eq 8b in the text.

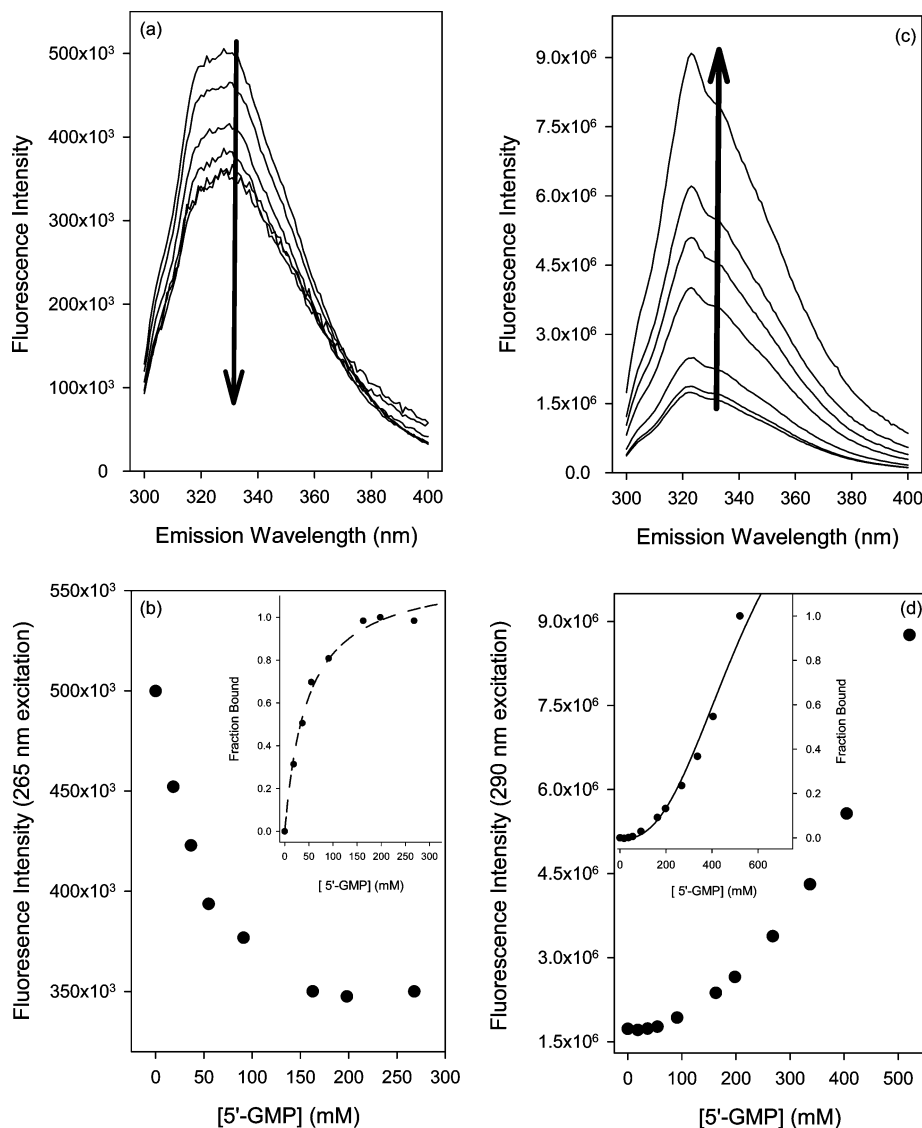


**Figure 3.** Dependence of the steady-state fluorescence of RNase t1 on 5'-GMP concentration. In all solutions, the reaction mixture was a solution containing 10 mM bis-tris and 10 mM NaCl buffered at pH 5.5. (a) Steady-state fluorescence spectrum of RNase t1 collected between 0 and 200  $\mu$ M 5'-GMP (following the arrow), with excitation at 265 nm and excitation and emission slits set to a 3 nm bandpass. (b) Fluorescence intensity of RNase t1 as a function of 5'-GMP concentration, with excitation at 265 nm, emission at 330 nm, and excitation and emission slits set to a 3 nm bandpass. For an explanation of the inset, refer to the text. (c) Steady-state fluorescence spectrum of RNase t1 collected between 0 and 500  $\mu$ M 5'-GMP (following the arrow), with excitation at 290 nm and excitation and emission slits set to a 3 nm bandpass. (d) Fluorescence intensity of RNase t1 as a function of 5'-GMP concentration, with excitation at 290 nm, emission at 330 nm, and excitation and emission slits set to a 3 nm bandpass. For an explanation of the inset, refer to the text.

spectrum of RNase t1 responds to the binding of competitive inhibitor guanosine 5'-monophosphate 5'-GMP to the protein. As may be observed in Figure 3b, the fluorescence spectrum of RNase t1 obtained from exciting the protein at 265 nm is quenched 5'-GMP exhibiting a hyperbolic dependence on concentration. From the quenching profile, the fraction of ligand-bound protein can be calculated via eq 2

$$\text{fraction of ligand-bound protein} = \frac{F - F_0}{F_{\max} - F_0} = f \quad (2)$$

where  $F_0$  is the protein fluorescence when no 5'-GMP has been added,  $F$  is the protein fluorescence at any 5'-GMP concentration, and  $F_{\max}$  is the protein fluorescence at the maximum 5'-GMP concentration. As shown in the inset,  $f$

follows a simple hyperbolic dependence on ligand concentration<sup>51</sup>

$$f = \frac{B[L]_{\text{free}}}{K_d + [L]_{\text{free}}} \quad (3)$$

where  $B$  is a constant,  $K_d$  is the binding constant, and  $[L]_{\text{free}}$  is the concentration of free ligand (in this case, 5'-GMP). From the inset data of Figure 3b,  $K_d = 50 \pm 7 \mu\text{M}$  and  $B_1 = 1.14 \pm 0.03$  are obtained from fitting the data to eq 3, consistent with values previously obtained in the literature.<sup>52,53</sup>

As observed in Figure 3c,d, the fluorescence spectrum of RNase t1 obtained from exciting the protein at 290 nm responds differently to 5'-GMP binding. The binding of 5'-GMP increases the fluorescence, and as observed in the inset of Figure 3d, the



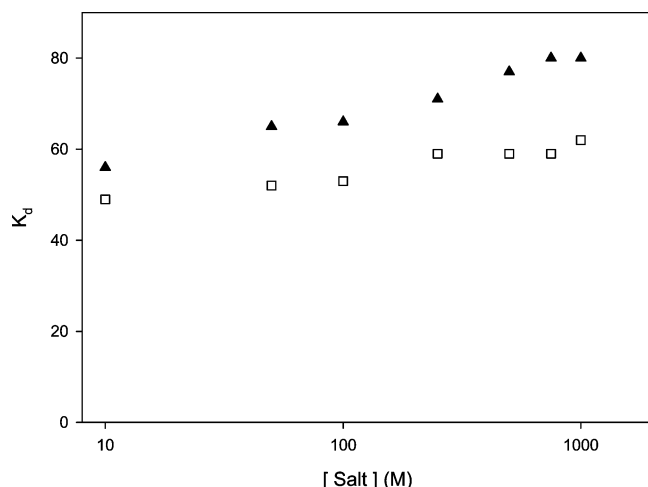


**Figure 4.** Effect of salt concentration on the  $K_d$  values for binding 5'-GMP to RNase t1. ( $\blacktriangle$ )  $K_d$  values measured in  $\text{MgCl}_2$  and ( $\square$ )  $K_d$  values measured in  $\text{NaCl}$ . In all cases, the reaction mixture contained 10 mM bis-tris and was buffered at pH 5.5.

parameter  $f$  does not follow a simple hyperbolic model but rather follows the sigmoidal Hill equation<sup>51</sup>

$$f = y_0 + \frac{a([L]_{\text{free}})^b}{(K_d)^b + ([L]_{\text{free}})^b} \quad (4)$$

where  $K_d$  is the apparent binding constant,  $[L]_{\text{free}}$  is the concentration of free ligand,  $a$  is a constant, and  $b$  is the cooperativity constant. From fitting the data in Figure 3d,  $K_d = 580 \pm 100 \mu\text{M}$  and  $b = 2.5 \pm 0.7$  are obtained. This result reaffirms that a secondary weakly binding site exists for the guanylyl moiety and that binding to this site is cooperatively linked to binding to the first site.<sup>53</sup>

The fluorescence results above indicate that by selectively exciting the tyrosine residues, properties of the primary binding site of the guanylyl moiety can be quantitatively probed with no interference from the second binding site. We have determined the salt effect on the binding of 5'-GMP to the primary site of RNase t1 by measuring fluorescence quenching profiles at various salt concentrations using an excitation wavelength of 255 nm. The data in Figure 4 show that increasing salt concentration has a small effect on the  $K_d$  of 5'-GMP binding to RNase t1, causing an increase of less than 35% upon addition of  $\text{MgCl}_2$  (the species having the largest effect on  $K_d$ ). Although they are not shown, measurements obtained from exciting the protein at 290 nm indicate that increasing salt concentrations have no appreciable effect on the binding affinity of 5'-GMP to the secondary binding site.

Finally, the effect of salt concentration on protein structure has been studied by acrylamide quenching of tryptophan fluorescence. Acrylamide quenching of tryptophan fluorescence was measured in solution containing  $0.5 \mu\text{M}$  RNase t1 in pH 5.5 buffer (10 mM bis-tris). The protein was excited at 290 nm, and the steady-state emission of the protein was monitored at 330 nm. The data in Figure 5 demonstrate that the addition of acrylamide quenches the protein fluorescence via the Stern–Volmer equation:<sup>50</sup>

$$\frac{I_0(330 \text{ nm})}{I(330 \text{ nm})} - 1 = K_{\text{SV}}C_{\text{AA}} = k_q\tau C_{\text{AA}} \quad (5)$$

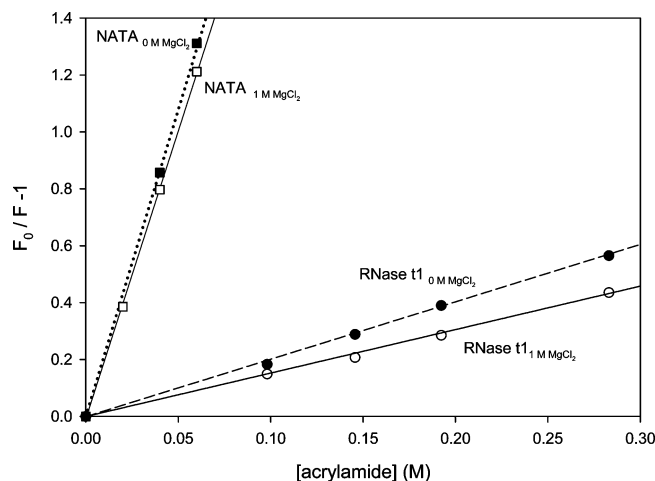


**Figure 5.** Stern–Volmer plots for the quenching of NATA ( $\square$ ,  $\blacksquare$ ) and RNase t1 ( $\circ$ ,  $\bullet$ ) fluorescence. The filled symbols were collected at 0 M  $\text{MgCl}_2$ , and the open circles were collected at 1 M  $\text{MgCl}_2$ . The excitation wavelength was set to 280 nm, and the emission was set to 330 nm. The excitation and emission slits were set to a 4 nm bandpass. In all cases, the concentration of fluorophor was set to  $0.5 \mu\text{M}$  and the reaction mixture contained 10 mM bis-tris and was buffered at pH 5.5.

In this equation,  $I_0$  is the RNase t1 tryptophan fluorescence intensity measured at 330 nm in the absence of acrylamide,  $I$  is the tryptophan fluorescence intensity of RNase t1 measured at a given acrylamide concentration,  $K_{\text{SV}}$  is the Stern–Volmer constant,  $k_q$  is the quenching constant,  $\tau$  is the tryptophan fluorescence lifetime measured in the absence of acrylamide, and  $C_{\text{AA}}$  is the concentration of acrylamide.

From the linear plot in Figure 5, a Stern–Volmer constant of  $2.02 \pm 0.04 \text{ M}^{-1}$  is obtained for RNase t1 under low salt conditions. However, when the same amount of protein is dissolved in pH 5.5 buffer (10 mM bis-tris) containing 1 M  $\text{MgCl}_2$ , the quenching efficiency of acrylamide decreases, resulting in a Stern–Volmer constant of  $1.53 \pm 0.04 \text{ M}^{-1}$ . This significant change in the Stern–Volmer constant indicates that the high concentration of salt has made the lone tryptophan of RNase t1 less accessible to solvent.<sup>50</sup> This is most likely due to the salt stabilizing a conformation of RNase t1 that has a more protected tryptophan.<sup>50</sup> As a control, the effect of  $\text{MgCl}_2$  on the fluorescence of *N*-acetyltryptophan amide (NATA) has also been investigated. Figure 5 shows the acrylamide quenching profile of  $0.5 \mu\text{M}$  NATA in pH 5.5 buffer (10 mM bis-tris) and in the same buffer solution containing 1 M  $\text{MgCl}_2$ . The plots show that the acrylamide quenching profile is minimally affected by the salt; the Stern–Volmer coefficient decreases from  $22 \pm 1$  to  $20 \pm 0.4 \text{ M}^{-1}$ ; this slight change is expected because the viscosity of the solution somewhat increases at high salt concentration. This observed insensitivity of NATA fluorescence toward  $\text{MgCl}_2$  agrees with our assumption that the salt-dependent decrease observed in the Stern–Volmer coefficient of RNase t1 is due to a change in protein properties rather than any interaction between the salt and tryptophan.

## Discussion

The data presented demonstrate that salts affect the catalytic efficiency of RNase t1. Traditionally, salt effects on enzyme catalytic properties have been analyzed on the basis of the following three possibilities: (1) the salt species affect the  $\text{p}K_a$  values of the active-site residues; (2) the salt species weaken

Coulombic interactions between the substrate and enzyme; and (3) the salt species bind directly to the enzyme, inhibiting the enzyme. The three possibilities have been examined in detail, and the following analysis has demonstrated that none of these three possibilities provide a satisfactory explanation of the observed salt effects on RNase t1 catalysis. We suggest that a fourth possibility may provide a more rational explanation of the observed salt effects, namely, that the observed salt effect is due to the salt species changing the hydrogen bonding properties of the water molecules of the protein solvent shell and thus indirectly stabilizing a less active conformation of the enzyme.

**Possibility 1: Salt Effect on  $pK_a$  Values of Active-Site Residues.** The residues histidine 40, histidine 92, glutamate 58, and an unidentified carboxylate have been identified as the major catalytic species in RNase t1.<sup>54,55</sup> Mechanistic studies on this enzyme have established that the protonation of both histidine residues is essential for maximal enzymatic activity. NMR studies have established that the  $pK_a$  values of H40 and H92 are respectively 7.7 and 7.4,<sup>54,55</sup> and values of 3.9 and 3.2 has been assigned to the  $pK_a$  of E58 and that of the unidentified carboxylate.<sup>54,55</sup> Extensive studies have established that salts do have a significant effect on histidine  $pK_a$  values (i.e., increasing the solvent salt concentration from 10 to 1 M will cause a significant increase in histidine  $pK_a$  values).<sup>56,57</sup> This increase in histidine  $pK_a$  will not cause a change in the protonation state of the catalytic imidazole rings at pH 5.5 and will therefore likely be a negligible component of the observed salt effect on  $k_{cat}/K_m$ . The effect of salts on the  $pK_a$  values of aspartate and glutamate has been studied in a number of protein systems, and it has been established as a rule of thumb that high salt concentrations change the  $pK_a$  values of these residues by about 0.3 to 0.7  $pK_a$  unit.<sup>58</sup> Upon the basis of this observation, even under high salt conditions both E58 and the unidentified carboxylate group will not be highly protonated at pH 5.5, supporting the suggestion that increasing the carboxylate  $pK_a$  is also not likely to be a significant component of the observed salt effect on  $k_{cat}/K_m$ .

**Possibility 2: Salt Species Weaken Coulombic Interactions between the Substrate and Enzyme (Counterion Effect).** Salts can dramatically affect substrate to enzyme binding if strong Coulombic interactions are major contributors to the substrate binding process.<sup>59–61</sup> In this case, as the substrate enters the enzyme binding pocket, strong electrostatic interactions between enzyme residues and the substrate molecule exclude substrate counterions from the vicinity of the substrate, causing the release of counterions into the bulk solvent. Thermodynamically, substrate counterion release becomes less favorable as salt concentration increases,<sup>62</sup> causing a commensurate decrease in substrate–enzyme affinity that will strongly affect the  $k_{cat}/K_m$  ratio. This counterion effect has been elegantly analyzed by Raines and co-workers,<sup>59–61</sup> leading to the following equation for the salt dependence of  $k_{cat}/K_m$

$$\frac{1}{\frac{k_{cat}}{K_m}} = \frac{1}{\left(\frac{k_{cat}}{K_m}\right)_{\max}} + \frac{[\text{salt}]^n}{\left(\frac{k_{cat}}{K_m}\right)_{1\text{ M}}} \quad (6)$$

where  $(k_{cat}/K_m)_{\max}$  is the value of  $k_{cat}/K_m$  limited by the encounter of the enzyme and substrate,  $(k_{cat}/K_m)_{1\text{ M}}$  is the value of  $k_{cat}/K_m$  at 1 M salt concentration, and  $n$  is a constant. In the special case when the enzyme is “sluggish” (i.e., the rate of substrate dissociation ( $k_{off}$ ) from the Michaelis complex is significantly

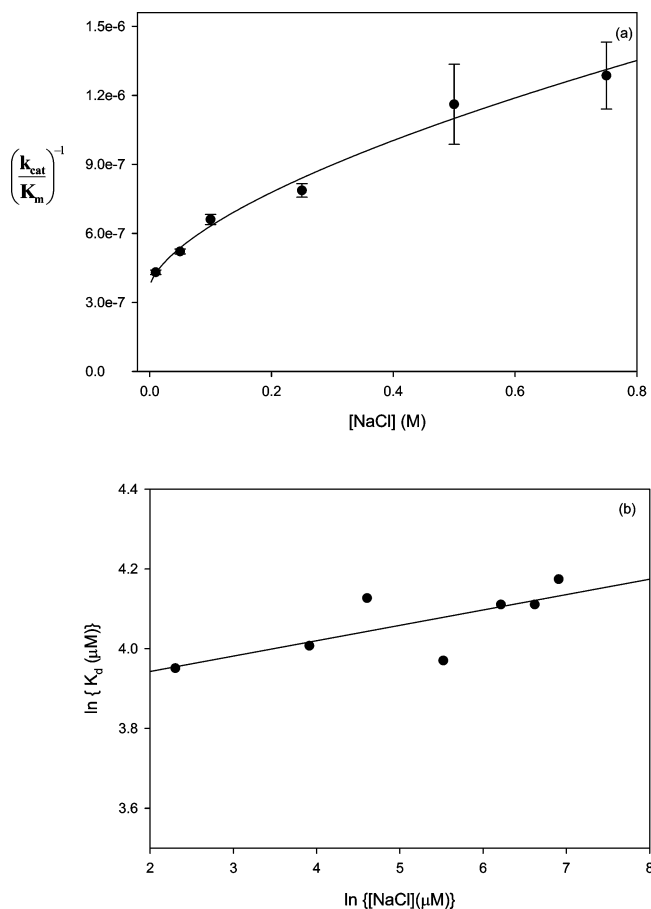


**Figure 6.** (a) Effect of NaCl on the parameter  $k_{cat}/K_m$  obtained from the enzyme-catalyzed hydrolysis of GpC. The solid line is obtained by fitting the data to eq 6 in the text. (b) Effect of NaCl on the  $K_d$  values obtained from the binding of 5'-GMP to RNase t1.

larger than the rate of catalysis ( $k_{cat}$ ), the value of  $n$  is close to the number of counterions released as the substrate binds enzyme. Enzymes that interact with their substrates via strong Coulombic interactions will release more than one counterion during substrate binding, leading to  $n$  values that are larger than 1.<sup>59–61,63</sup>

In Figure 6a, we have replotted the data in Figure 2a (NaCl) in order to fit the data to eq 6. From the fit, a value of  $0.6 \pm 0.2$  is obtained for the  $n$  parameter. The fact that this value of  $n$  is significantly lower than 1 indicates that the interaction of GpC with RNase t1 is not dominated by Coulombic forces, consistent with the work of Walz<sup>64</sup> in his initial investigations regarding this enzyme. This lack of dominant Coulombic interactions hints that our observed salt effects are not likely to be due to counterion release. The investigations with the binding of 5'-GMP to RNase t1 provide further evidence against assigning the observed salt effect to counterion release. The GpC and 5'-GMP species have the same formal charge on their phosphate groups at pH 5.5; therefore, to a first approximation both species would have a similar number of counterions ( $n'$ ) associated with them. Upon the basis of the Raines formalism,<sup>59–61</sup> the salt effect upon the  $K_d$  should be

$$\frac{\partial(\log K_d)}{\partial(\log[\text{salt}])} = n' \quad (7)$$

From temperature-jump kinetics experiments done on substrate-mimicking ligands,<sup>53,65</sup> the  $k_{off}$  value of GpC can be estimated

**TABLE 1: Values of the  $K$  Parameter Associated with RNase t1 for Each Data Set Depicted in Figure 2**

| salt     | $K$ ( $M^{-1}$ ) |
|----------|------------------|
| NaCl     | $8 \pm 2$        |
| KCl      | $8.6 \pm 0.8$    |
| LiCl     | $13 \pm 1$       |
| $NH_4Cl$ | $16 \pm 3$       |
| $CaCl_2$ | $14.0 \pm 0.7$   |
| $MgCl_2$ | $21 \pm 3$       |

to be larger than  $2000\ s^{-1}$  and the  $k_{cat}$  values for the enzyme using GpC are in the lower hundreds of inverse seconds. These values indicate that RNase t1 is a sluggish enzyme for the GpC substrate. Therefore, the value of  $n$  obtained from eq 6 should be close to  $n'$ . In Figure 6b, we have replotted the data from Figure 4 to fit eq 7. Our correlation yields  $n' = 0.04 \pm 0.02$ , which is significantly different from  $n$ . The small value of  $n'$  for 5'-GMP binding demonstrates that the binding of substrate-mimicking ligands to the enzyme is not accompanied by significant counterion release. In addition, the large difference observed between the  $n$  value obtained from Figure 6a and  $n'$  indicates that the origin of the observed salt dependence of  $k_{cat}/K_m$  is not simple substrate-binding thermodynamics. Therefore, counterion release can likely be ruled out as a possible mechanism for the observed salt effects.

**Possibility 3: Metal Cations Bind Directly to the Enzyme, Thereby Inhibiting the Enzyme.** Traditionally, salt effects on enzyme activity have been analyzed by treating one of the ionic components of the salt as an enzyme inhibitor.<sup>66</sup> This treatment implicitly assumes that salt components directly bind to a specific site on the enzyme and consequently stabilize a less active enzyme conformation, which results in the loss of enzyme activity (eqs 8a and 8b):



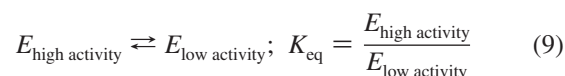
$$\left(\frac{k_{cat}}{K_m}\right)_{obsd} = \frac{\left(\frac{k_{cat}}{K_m}\right)_{low\ salt} + Kc\left(\frac{k_{cat}}{K_m}\right)_{high\ salt}}{1 + Kc} \quad (8b)$$

In this formalism,  $E_{low\ salt}$  is the enzyme in the active low-salt form,  $E_{ion}$  is the enzyme in the less active bound-to-ion form,  $(k_{cat}/K_m)_{obsd}$  is the specificity constant observed at any given salt concentration,  $(k_{cat}/K_m)_{low\ salt}$  is the specificity constant of the active low-salt form of the enzyme,  $(k_{cat}/K_m)_{high\ salt}$  is the specificity constant of the ion-bound form of the enzyme,  $K$  is the equilibrium binding constant of the ion to the enzyme, and  $c$  is the formal concentration of salt.

Upon the basis of the fluorescence quenching data shown in Figure 5, it is reasonable to conclude that high salt concentrations force a conformational change in the RNase t1 enzyme. This allows us to analyze the data in Figure 2 on the basis of eqs 8a and 8b. The data in Figure 2 have been fitted to eq 8b, and it can be observed that the data are well correlated with eq 8b with reasonable  $r^2$  values (greater than 0.99). We have tabulated the values of the  $K$  parameter for each set of data in Table 1. The  $K$  values of LiCl, NaCl,  $NH_4Cl$ , and KCl and those of  $MgCl_2$  and  $CaCl_2$  differ from each other, indicating that according to eqs 8a and 8b the cation species are the inhibitors. In Table 1, we observe that the values of  $K$  vary between 8 and  $21\ M^{-1}$ ; from these  $K$  values, a free energy of interaction of about 5–7.5 kJ/mol is estimated.

The fact that the values of  $K$  are small presents an interesting dilemma on how to interpret the nature of the interaction between salt species and the enzyme. Whereas in the case of strongly interacting ligands (ligands interacting with enzyme at submillimolar concentrations) it is valid to assume localized interaction sites on the enzyme and model the interaction as a site-specific binding process, it has been definitively shown that such models are inapplicable to ligands that weakly interact with enzymes<sup>67,68</sup> and applying site-specific binding models to weak ligand–protein interactions often leads to ambiguous and erroneous results.<sup>69</sup> In this particular case, the model assumes that RNase t1 has a specific metal ion binding site on its surface. It has been suggested that by analogy to zinc and other heavy atoms that bind to RNase t1 at the micromolar level<sup>70,71</sup> divalent cations also bind to a specific surface carboxylate residue, asp49.<sup>72</sup> If this is the case, then the binding of  $Mg^{2+}$  to RNase t1 with a binding constant of  $21\ M^{-1}$  should stabilize the protein by approximately 7.5 kJ/mol. If asp 49 is mutated to alanine, then the binding site is lost; therefore, the mutant protein dissolved in 1 M  $MgCl_2$  should be destabilized by at least 7.5 kJ/mol relative to the wild type. The free energy of unfolding ( $\Delta G_{unfolding}^0$ ) for the wild-type RNase t1 in the absence of salt is 24.2 kJ/mol, and in 1 M  $MgCl_2$ , it is 43.7 kJ/mol, with the salt inducing a stability of  $\sim 20$  kJ/mol. Mutating any of the surface carboxylates (including asp49) does not reduce the  $\Delta G_{unfolding}^0$  value of the protein by anything more than 2 kJ/mol in 1 M  $MgCl_2$ .<sup>72</sup> These results are inconsistent with a specific binding site model. Although it is still reasonable to assume that a high concentration of salt forces the enzyme into a less active compact form, it is very unlikely that this conformational change is mediated through cation (or anion) binding to a specific site on the enzyme.

**Possibility 4: Observed Salt Effect Is Due to the Salt Species Changing the Hydrogen Bonding Properties of the Water Molecules of the Protein Solvent Shell, Thus Indirectly Stabilizing a Less Active Conformation of the Enzyme.** Salt species can also change the properties of the hydration layer of proteins and thus affect the thermodynamic properties of proteins.<sup>41–44</sup> If this premise is accepted, then salt effects on enzyme activity can be modeled by assuming that the enzyme at all times is in equilibrium between conformers of high and low catalytic activity (eq 9):



The addition of salt causes a shift in this equilibrium; therefore,  $K_{eq}$  can be represented as a polynomial function of salt concentration (eq 10) where  $c$  is the concentration of salt and  $K_n$  is a constant:

$$K_{eq} = \sum_0^n K_n c^n \quad (10)$$

As a first approximation, let us assume that  $K_{eq} \approx K_0 + Kc$ , in which case the measured enzyme activity will then be

$$\begin{aligned}
 \left(\frac{k_{\text{cat}}}{K_m}\right)_{\text{obsd}} &= \frac{\left(\frac{k_{\text{cat}}}{K_m}\right)_{\text{high activity}} + (K_0 + Kc)\left(\frac{k_{\text{cat}}}{K_m}\right)_{\text{low activity}}}{1 + (K_0 + Kc)} \\
 &= \frac{\left(\frac{k_{\text{cat}}}{K_m}\right)_{\text{high activity}} + K_0\left(\frac{k_{\text{cat}}}{K_m}\right)_{\text{low activity}} + Kc\left(\frac{k_{\text{cat}}}{K_m}\right)_{\text{low activity}}}{1 + (K_0 + Kc)} \\
 &= \frac{\left(\frac{k_{\text{cat}}}{K_m}\right)_{\text{high activity}} + K_0\left(\frac{k_{\text{cat}}}{K_m}\right)_{\text{low activity}} + Kc\left(\frac{k_{\text{cat}}}{K_m}\right)_{\text{low activity}}}{1 + (K_0 + Kc)} \\
 &= \frac{\left(\left(\frac{k_{\text{cat}}}{K_m}\right)_{\text{high activity}} + K_0\left(\frac{k_{\text{cat}}}{K_m}\right)_{\text{low activity}}\right)\frac{1}{1 + K_0} + \frac{Kc\left(\frac{k_{\text{cat}}}{K_m}\right)_{\text{low activity}}}{1 + K_0}}{1 + \frac{K}{1 + K_0}c}
 \end{aligned}$$

Rearranging the above equation yields the following:

$$\left(\frac{k_{\text{cat}}}{K_m}\right)_{\text{obsd}} = \frac{\left(\frac{k_{\text{cat}}}{K_m}\right)_{\text{obsd at low salt}} + c\left(\frac{K}{1 + K_0}\right)\left(\frac{k_{\text{cat}}}{K_m}\right)_{\text{low activity}}}{1 + \left(\frac{K}{1 + K_0}\right)c} \quad (11)$$

This equation has the same form as eq 8b, and because reasonable correlations are obtained from fitting the data to eq 11, it can be concluded that the linear approximation is valid. Therefore, the  $K$  values reported in Table 1 should more correctly be designated as  $K/(1 + K_0)$ . Variations between  $K/(1 + K_0)$  values associated with different monovalent and divalent salts indicate that  $K$  is not merely a function of ionic strength but instead point out that  $K$  is salt-specific, ruling out polyelectrolyte repulsion screening<sup>73,74</sup> as the only contributor to stabilizing the low-activity form of the enzyme. If our observed salt effects significantly depend upon how the salt species change the hydrogen bonding properties of the water molecules of the protein solvent shell, then  $K$  should depend upon how each different ionic salt species interacts with water.

One method of characterizing salt–water interactions is measuring the effect that dissolving salt has upon solvent viscosity.<sup>75</sup> The viscosities of aqueous solutions of strong electrolytes exhibit the following concentration dependence (the Jones–Dole equation)<sup>75</sup>

$$\frac{\eta}{\eta_0} = 1 + A\sqrt{c} + Bc \quad (12)$$

where  $\eta$  is the viscosity of a salt solution and  $\eta_0$  is the viscosity of pure water at the same temperature,  $c$  is the salt concentration,  $A$  is an electrostatic term that is essentially 1 for moderate salt concentrations, and  $B$  depends upon the ratio of the strength of ion–water interactions to the strength of water–water interactions in bulk solution (positive  $B$  coefficients for strongly hydrated ions and negative  $B$  coefficients for weakly hydrated ions). Coefficient  $B$  can be expressed as  $B = B_{(+)} + B_{(-)}$  in which  $B_{(\pm)}$  is the contribution of the ion of each salt. Using the values of Marcus for the  $B_{(\pm)}$  coefficients, we have plotted  $K/(1 + K_0)$  as a function of the Jones–Dole  $B$  parameter in Figure 7a. The data demonstrate that with the exception of  $\text{NH}_4\text{Cl}$ , the

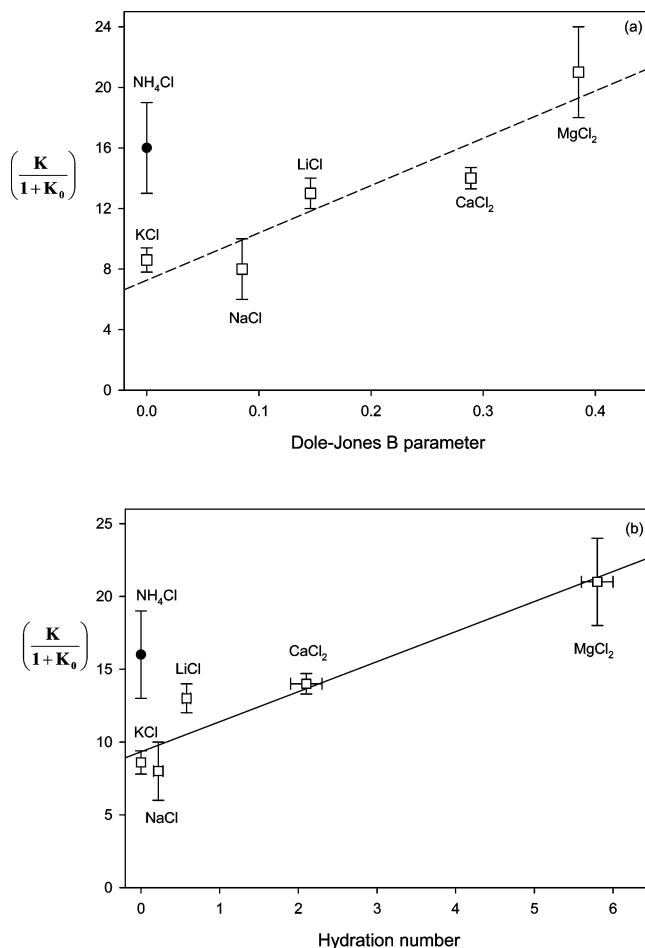


**Figure 7.** (a) Dependence of the  $K/(1 + K_0)$  parameter of RNase t1 upon the Jones–Dole  $B$  parameter of various salts. The dotted line is the linear regression line run through the data associated with the metal chloride salts. (b) Dependence of the  $K/(1 + K_0)$  parameter upon the cation hydration numbers of various salts obtained from refs 62 and 63. The solid line is the linear regression line run through the data associated with the metal chloride salts.

$K/(1 + K_0)$  values of all other salts effectively correlate with cation  $B_{(+)}$  values (for chloride,  $B_{(-)} = -0.007$ ).

Alternatively the strength of ion–water interactions can also be determined using chromatographic and interfacial methods.<sup>76,77</sup> These interactions have been characterized by assigning hydration numbers (the number of tightly bound water molecules that move with an ion as it diffuses) to various ions. We have plotted  $K/(1 + K_0)$  as a function of the hydration number of each salt cation in Figure 7b, and again we observe that the  $K/(1 + K_0)$  values correlate with the cation hydration value (with the exception of  $\text{NH}_4\text{Cl}$ ). Indeed, if ammonium chloride is ignored we observe

$$\left(\frac{K}{1 + K_0}\right)_{\text{Mg}^{2+}} > \left(\frac{K}{1 + K_0}\right)_{\text{Ca}^{2+}} > \left(\frac{K}{1 + K_0}\right)_{\text{Li}^{+}} > \left(\frac{K}{1 + K_0}\right)_{\text{Na}^{+}} \approx \left(\frac{K}{1 + K_0}\right)_{\text{K}^{+}}$$

These values follow the kosmotrope ordering of cations in the Hofmeister series,<sup>43</sup> suggesting that salts may indeed affect the properties of RNase t1 by perturbing the properties of water molecules.



A major problem with all hydration parameters used in our correlations above is that they are determined from changes in bulk macroscopic properties of aqueous solutions. More meaningful correlations can be obtained if  $K/(1 + K_0)$  values are correlated with parameters that probe water hydrogen bonding properties at the molecular level. According to the two-state model, liquid water can be considered to be a mixture of two states at equilibrium with one another: the highly ordered low-density water state ( $\text{water}_{\text{LD}}$ ) consisting mostly of water molecules interacting via high-angle linear hydrogen bonds and the less-ordered high-density state consisting of water molecules interacting with one another via nonregular bent tetrahedral hydrogen bonding ( $\text{water}_{\text{HD}}$ ). The two kinds of hydrogen bonding give rise to different signatures in the vibrational spectrum of water.<sup>78</sup> Vanderkooi has characterized the effects of salts upon the different hydrogen bonding interactions of water using temperature excursion IR spectroscopy in aqueous salt solutions having a concentration of 4.4 *m*.<sup>79</sup> At this concentration, 55 molecules of water are present per molecule of ion; therefore, each ion is solvated by only a few solvation layers of water molecules. As a first approximation, the water molecules in this experiment can then be considered to be representative of water molecules in the vicinity of ions in solution. By applying a two-state hydrogen bonding model to interpret the temperature excursion infrared response of the O–H stretch of aqueous salt solutions, we can write



Vanderkooi<sup>79</sup> has determined the perturbations by different salt species on the equilibrium described in eq 13, characterizing these perturbations by an effective free-energy difference ( $\Delta G^\circ$ ), between  $\text{water}_{\text{HD}}$  and  $\text{water}_{\text{LD}}$  (i.e., between bent and linear hydrogen bonds). The  $\Delta G^\circ$  value for eq 13 in pure water is 250  $\text{cal M}^{-1}$ , and the  $\Delta G^\circ$  values for different solutions of 4.4 *m* salt (in  $\text{cal M}^{-1}$ ) are<sup>79</sup> 55 $_{\text{MgCl}_2}$ , 244 $_{\text{NH}_4\text{Cl}}$ , 250 $_{\text{CaCl}_2}$ , 278 $_{\text{LiCl}}$ , 437 $_{\text{KCl}}$ , and 448 $_{\text{NaCl}}$ .

These values can be interpreted using the results of Dill and co-workers regarding the solvation of ionic species in water using the Mercedes-Benz (MB) model for molecular water.<sup>80,81</sup> Dill has demonstrated that small ions order first-shell water molecules through an electrostatic mechanism, disrupting hydrogen bonding among first hydration shell water molecules and orienting them in the  $\text{water}_{\text{HD}}$  form.<sup>80,81</sup> Increasing the cation size diminishes the electrostatic interaction of the ion on nearby water molecules. The ordering of water molecules around larger cations has a larger contribution from water–water hydrogen bonding. Therefore, as the sizes of the cations increase, the water molecules of their first solvation shell lose  $\text{water}_{\text{HD}}$  character and approach the behavior of water molecules present near nonpolar solutes.<sup>81</sup> These results imply that because small ions cause an increase in  $\text{water}_{\text{HD}}$  concentration in the first ion solvation shell, the equilibrium in eq 13 will force water molecules in the subsequent shells to adopt  $\text{water}_{\text{LD}}$  conformations. Therefore, the salt  $\Delta G^\circ$  values indicate the ability of the salts to induce water molecules to adopt  $\text{water}_{\text{LD}}$  conformations beyond their first solvation shell. For example, the  $\Delta G^\circ$  values for pure water and a 4.4 *m* solution of  $\text{CaCl}_2$  are practically equal; however, because the  $\text{Ca}^{2+}$  ion has a high charge density, it will orient most of its first-shell water molecules in the  $\text{water}_{\text{HD}}$  form. As a consequence, on the basis of equilibrium considerations, a much larger fraction of water molecules in the subsequent solvation shells of  $\text{Ca}^{2+}$  will adopt the  $\text{water}_{\text{LD}}$  conformation in comparison to pure water. In fact, Bakker and

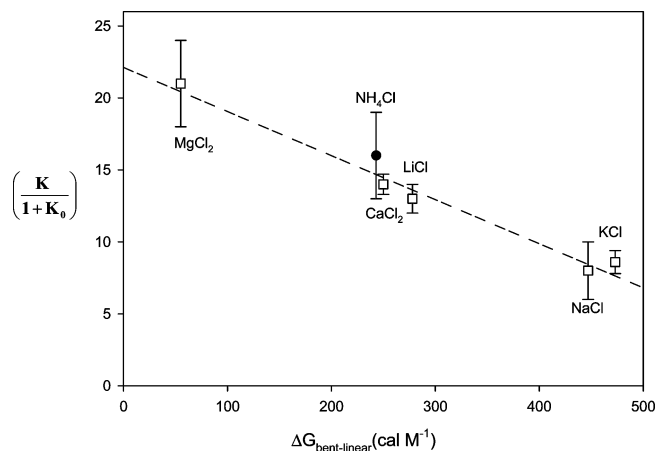


**Figure 8.** Dependence of the  $K/(1 + K_0)$  parameter of RNase t1 upon the effective free-energy difference ( $\Delta G^\circ$ ) between  $\text{water}_{\text{HD}}$  and  $\text{water}_{\text{LD}}$  of various 4.4 *m* salt solutions.

co-workers have demonstrated that salts such as  $\text{MgCl}_2$  and  $\text{MgSO}_4$  are able to “order water molecules far beyond their first solvation shell”,<sup>82</sup> confirming that these ions stabilize the formation of  $\text{water}_{\text{LD}}$  in solvation layers beyond the first solvation shell. This stabilization of  $\text{water}_{\text{LD}}$  prevents the solubilization of nonpolar groups in water<sup>80</sup> because the solvation of hydrophobic moieties requires a population of  $\text{water}_{\text{LD}}$  molecules that can be readily converted to  $\text{water}_{\text{HD}}$ ,<sup>21</sup> hence hydrophobic interactions are enhanced when salts promoting  $\text{water}_{\text{LD}}$  are dissolved in water.

Figure 8 plots  $K/(1 + K_0)$  as a function of  $\Delta G^\circ$  of the 4.4 *m* salt solutions. As can be observed, the metal chloride values of  $K/(1 + K_0)$  are well correlated with  $\Delta G^\circ$ ; however, in contrast to our other correlations in Figure 7, the data point associated with  $\text{NH}_4\text{Cl}$  also follows the correlation, suggesting that  $\text{NH}_4\text{Cl}$  is also capable of promoting the formation of  $\text{water}_{\text{LD}}$ . This underlines the role that the chloride counterion plays in ordering water molecules: the effects of ions and counterions have been shown to be “strongly interdependent and nonadditive”,<sup>43,82</sup> therefore, how strongly a particular ion affects water dynamics is enhanced by the presence of its counterion.<sup>43,82</sup>

Upon the basis of the correlation in Figure 8, we can offer the following explanation for the observed salt effects on the reactivity of RNase t1. Because the enzyme has six positively charged and nine negatively charged residues at pH 5.5, electrostatic interactions will cause ions of opposite charge be attracted to these residues, leading to the migration of these species to the hydration layer of the protein and enriching the local concentration of ions in the vicinity of the protein relative to that of the bulk solvent. This partitioning of ionic species in the protein hydration layer (especially the cations) will perturb the hydrogen bonding network, shifting the equilibrium between  $\text{water}_{\text{HD}}$  and  $\text{water}_{\text{LD}}$ . Cations with a high charge density promote the formation of  $\text{water}_{\text{LD}}$  in the protein hydration layer, enhancing hydrophobic interactions and thereby causing a more compact, rigid, and less active form of RNase t1 to be stabilized. This stabilization leads to the observed loss in enzyme activity as the bulk salt concentration increases.

It must be emphasized that the manifestation of these salt effects does not require a nonphysiological concentration of salt. For example, the hydration layer of a protein such as RNase t1 contains approximately 250 water molecule.<sup>33</sup> If one of these water molecules is replaced by one formal unit of  $\text{MgCl}_2$ , then a local concentration of 0.2 M salt is obtained. However, this replacement will affect 55 molecules of water,<sup>79</sup> which is the

hydrogen bonding of at least 20% of the water molecules of the protein hydration layer. This will perturb the thermodynamic properties of the protein. Our results present a new challenge for theoreticians modeling protein structures in solution because they demonstrate that the hydration layer of proteins under physiological conditions may be very different that from that of proteins in pure water.

## Conclusions

In this work, the effects of various simple salts upon the catalytic activity of RNase t1 has been studied. The data demonstrate that these effects cannot be well explained by the following assumptions: the salt is affecting the  $pK_a$  values of the active-site residues; the salt species are weakening Coulombic interactions between the substrate and enzyme; and the salt species affect the enzyme through simple inhibition mechanisms. The data also demonstrate that increasing the amount of salt in the protein solvent promotes a more compact, less active form of the enzyme and that the ability of each salt species to promote the formation of the less active species of the enzyme is correlated with its ability to promote icelike hydrogen bonding through the water network. Because in addition to charge screening, salts can also affect the hydrogen bonding network of water, we suggest the following explanation for our observed salt effects based on the two-phase model for liquid water: salts perturb the protein hydration layer by shifting the equilibrium between water<sub>HD</sub> and water<sub>LD</sub>; because various conformations of the protein interact differently with the two kinds of water, this shift in equilibrium will stabilize one protein conformation over others. In this study, our results are compatible with the assumption that water<sub>LD</sub> stabilizes a compact form of RNase t1.

**Acknowledgment.** This work was supported in part by University of Manitoba UMRG funding. We thank Dr. Joe O'Neil and Dr. Sean McKenna (University of Manitoba), Dr. Camille Roche and Dr. Joel Friedman (The Albert Einstein College of Medicine), Dr. Kim Sharp (University of Pennsylvania), and Dr. Wayne Bolen (University of Texas) for informative discussions regarding this article.

## Abbreviations

|                     |  |
|---------------------|--|
| RNase t1            | ribonuclease t1 from <i>Aspergillus oryzae</i> |
| 5-GMP               | guanylyl-5' monophosphate                      |
| GpC                 | guanylyl-3' → 5'-cytidine                      |
| NATA                | <i>N</i> -acetyl-L-tryptophanamide             |
| W59                 | tryptophan 59 of RNase t1                      |
| water <sub>LD</sub> | highly-ordered low density water               |
| water <sub>HD</sub> | less-ordered high-density water                |

## References and Notes

- (1) Cornish-Bowden, A. *Fundamentals of Enzyme Kinetics*, 3rd ed.; Portland Press: London, 2004.
- (2) Koshland, D. E., Jr. *Science* **1963**, *142*, 1533.
- (3) Wolfenden, R.; Radzicka, A. *Curr. Opin. Struct. Biol.* **1991**, *1*, 780.
- (4) Schowen, R. L. *Proc. Natl. Acad. Sci. U.S.A.* **2003**, *100*, 11931.
- (5) Schramm, V. L. *Arch. Biochem. Biophys.* **2005**, *433*, 13.
- (6) Fersht, A. R. *Proc. Robert A. Welch Found. Conf. Chem. Res.* **1987**, *31*, 158.
- (7) Callender, R.; Dyer, R. B. *Curr. Opin. Struct. Biol.* **2002**, *12*, 628.
- (8) Schnell, J. R.; Dyson, H. J.; Wright, P. E. *Annu. Rev. Biophys. Biomol. Struct.* **2004**, *33*, 119.
- (9) Hammes, G. G. *Biochemistry* **2002**, *41*, 8221.
- (10) Franks, F. *Protein Biotechnol.* **1993**, *437*.
- (11) Frauenfelder, H.; Chen, G.; Berendzen, J.; Fenimore, P. W.; Jansson, H.; McMahon, B. H.; Strope, I. R.; Swenson, J.; Young, R. D. *Proc. Natl. Acad. Sci. U.S.A.* **2009**, *106*, 5129.
- (12) Zhong, D. *Adv. Chem. Phys.* **2009**, *143*, 83.

- (13) Reategui, E.; Aksan, A. *Phys. Chem. Chem. Phys.*, *12*, 10161.
- (14) Lusceac, S. A.; Vogel, M. *J. Phys. Chem. B*, *114*, 10209.
- (15) Khodadadi, S.; Roh, J. H.; Kisliuk, A.; Mamontov, E.; Tyagi, M.; Woodson, S. A.; Briber, R. M.; Sokolov, A. P. *Biophys. J.*, *98*, 1321.
- (16) LeBard, D. N.; Matyushov, D. V. *Phys. Rev. E: Stat., Nonlinear, Soft Matter Phys.* **2008**, *78*, 061901/1.
- (17) Frauenfelder, H.; Fenimore, P. W.; Chen, G.; McMahon, B. H. *Proc. Natl. Acad. Sci. U.S.A.* **2006**, *103*, 15469.
- (18) Buckingham, A. D.; Del Bene, J. E.; McDowell, S. A. *Chem. Phys. Lett.* **2008**, *463*, 1.
- (19) Sharp, K. A.; Vanderkooi, J. M. *Acc. Chem. Res.* **2010**, *43*, 231.
- (20) Sharp, K. A.; Madan, B.; Manas, E.; Vanderkooi, J. M. *J. Chem. Phys.* **2001**, *114*, 1791.
- (21) Robinson, G. W.; Cho, C. H. *Biophys. J.* **1999**, *77*, 3311.
- (22) Graziano, G.; Lee, B. *J. Phys. Chem. B* **2005**, *109*, 8103.
- (23) Dillon, S. R.; Dougherty, R. C. *J. Phys. Chem. A* **2002**, *106*, 7647.
- (24) Chalikian, T. V. *J. Phys. Chem. B* **2001**, *105*, 12566.
- (25) Wiggins, P. *PLoS One* **2008**, *3*, e1406.
- (26) Tanaka, H. *J. Chem. Phys.* **2000**, *112*, 799.
- (27) Binder, H. *Eur. Biophys. J.* **2007**, *36*, 265.
- (28) Urquidí, J.; Cho, C. H.; Singh, S.; Robinson, G. W. *J. Mol. Struct.* **1999**, *485–486*, 363.
- (29) Hayashi, Y.; Katsumoto, Y.; Omori, S.; Kishii, N.; Yasuda, A. *J. Phys. Chem. B* **2007**, *111*, 1076.
- (30) Guttman, H. J.; Anderson, C. F.; Record, M. T., Jr. *Biophys. J.* **1995**, *68*, 835.
- (31) Der, A.; Kelemen, L.; Fabian, L.; Taneva, S. G.; Fodor, E.; Pali, T.; Cupane, A.; Cacace, M. G.; Ramsden, J. J. *J. Phys. Chem. B* **2007**, *111*, 5344.
- (32) Mattea, C.; Qvist, J.; Halle, B. *Biophys. J.* **2008**, *95*, 2951.
- (33) Timasheff, S. N. *Biochemistry* **2002**, *41*, 13473.
- (34) Zhang, L.; Yang, Y.; Kao, Y.-T.; Wang, L.; Zhong, D. *J. Am. Chem. Soc.* **2009**, *131*, 10677.
- (35) Schiro, G.; Cupane, A.; Vitrano, E.; Bruni, F. *J. Phys. Chem. B* **2009**, *113*, 9606.
- (36) Zhang, H.; Annunziata, O. *Phys. Chem. Chem. Phys.* **2009**, *11*, 8923.
- (37) Arakawa, T.; Kita, Y.; Timasheff, S. N. *Biophys. Chem.* **2007**, *131*, 62.
- (38) Shah, P. P.; Roberts, C. J. *J. Phys. Chem. B* **2007**, *111*, 4467.
- (39) Yamazaki, T.; Imai, T.; Hirata, F.; Kovalenko, A. *J. Phys. Chem. B* **2007**, *111*, 1206.
- (40) Roche, C. J.; Guo, F.; Friedman, J. M. *J. Biol. Chem.* **2006**, *281*, 38757.
- (41) Cappa, C. D.; Smith, J. D.; Wilson, K. R.; Messer, B. M.; Gilles, M. K.; Cohen, R. C.; Saykally, R. J. *J. Phys. Chem. B* **2005**, *109*, 7046.
- (42) Smith, J. D.; Saykally, R. J.; Geissler, P. L. *J. Am. Chem. Soc.* **2007**, *129*, 13847.
- (43) Guo, F.; Friedman, J. M. *J. Am. Chem. Soc.* **2009**, *131*, 11010.
- (44) Thomas, A. S.; Elcock, A. H. *J. Am. Chem. Soc.* **2007**, *129*, 14887.
- (45) Moelbert, S.; Normand, B.; De Los Rios, P. *Biophys. Chem.* **2004**, *112*, 45.
- (46) Pace, C. N.; Grimsley, G. R. *Biochemistry* **1988**, *27*, 3242.
- (47) Steyaert, J.; Wyns, L.; Stanssens, P. *Biochemistry* **1991**, *30*, 8661.
- (48) Kumar, K.; Walz, F. G., Jr. *Biochemistry* **2001**, *40*, 3748.
- (49) Du, H.; Fuh, R.-C. A.; Li, J.; Corkan, L. A.; Lindsey, J. S. *Photochem. Photobiol.* **1998**, *68*, 141.
- (50) Lakowicz, J. R. *Principles of Fluorescence Spectroscopy*; Plenum Press: New York, 1983.
- (51) Cantor, C. R.; Schimmel, P. R. *The Behavior of Biological Macromolecules*; Their Biophysical Chemistry, Pt. 3; W. H. Freeman: San Francisco, 1980.
- (52) Hu, C. Q.; Sturtevant, J. M. *J. Phys. Chem.* **1992**, *96*, 4052.
- (53) Georgalis, Y.; Zouni, A.; Zielenkiewicz, P.; Holzwarth, J. F.; Clarke, R.; Hahn, U.; Saenger, W. *J. Biol. Chem.* **1992**, *267*, 10323.
- (54) Osterman, H. L.; Walz, F. G., Jr. *Biochemistry* **1979**, *18*, 1984.
- (55) Steyaert, J.; Hallenga, K.; Wyns, L.; Stanssens, P. *Biochemistry* **1990**, *29*, 9064.
- (56) Kao, Y.-H.; Fitch, C. A.; Bhattacharya, S.; Sarkisian, C. J.; Lecomte, J. T. J.; Garcia-Moreno, E. B. *Biophys. J.* **2000**, *79*, 1637.
- (57) Lee, K. K.; Fitch, C. A.; Lecomte, J. T. J.; Garcia-Moreno, E. B. *Biochemistry* **2002**, *41*, 5656.
- (58) Abe, Y.; Ueda, T.; Iwashita, H.; Hashimoto, Y.; Motoshima, H.; Tanaka, Y.; Imoto, T. *J. Biochem.* **1995**, *118*, 946.
- (59) Park, C.; Raines, R. T. *J. Am. Chem. Soc.* **2001**, *123*, 11472.
- (60) Fisher, B. M.; Schultz, L. W.; Raines, R. T. *Biochemistry* **1998**, *37*, 17386.
- (61) Park, C.; Raines, R. T. *FEBS Lett.* **2000**, *468*, 199.
- (62) Record, M. T., Jr.; Lohman, T. M.; De Haseth, P. *J. Mol. Biol.* **1976**, *107*, 145.
- (63) Korenykh, A. V.; Piccirilli, J. A.; Correll, C. C. *Nat. Struct. Mol. Biol.* **2006**, *13*, 436.
- (64) Walz, F. G., Jr. *Biochemistry* **1977**, *16*, 5509.

- (65) Walz, F. G., Jr. *Biochim. Biophys. Acta, Protein Struct. Mol. Enzymol.* **1992**, 1159, 327.
- (66) Bowers, E. M.; Ragland, L. O.; Byers, L. D. *Biochim. Biophys. Acta, Proteins Proteomics* **2007**, 1774, 1500.
- (67) Timasheff, S. N. *Biophys. Chem* **2002**, 101–102, 99.
- (68) Schellman, J. A. *Biopolymers* **1994**, 34, 1015.
- (69) Schellman, J. A. *Biophys. Chem.* **1993**, 45, 273.
- (70) Itaya, M.; Inoue, Y. *Biochem. J.* **1982**, 207, 357.
- (71) Ding, J.; Choe, H. W.; Granzin, J.; Saenger, W. *Acta Crystallogr., Sect. B: Struct. Sci.* **1992**, B48, 185.
- (72) Deswarte, J.; De Vos, S.; Langhorst, U.; Steyaert, J.; Loris, R. *Eur. J. Biochem.* **2001**, 268, 3993.
- (73) Higgs, P. G.; Joanny, J. F. *J. Chem. Phys.* **1991**, 94, 1543.
- (74) Ciferri, A. *Biopolymers* **2008**, 89, 700.
- (75) Jenkins, H. D. B.; Marcus, Y. *Chem. Rev.* **1995**, 95, 2695.
- (76) Schlenoff, J. B.; Rmaile, A. H.; Bucur, C. B. *J. Am. Chem. Soc.* **2008**, 130, 13589.
- (77) Kiriukhin, M. Y.; Collins, K. D. *Biophys. Chem.* **2002**, 99, 155.
- (78) Walrafen, G. E. *J. Chem. Phys.* **2004**, 120, 4868.
- (79) Nucci, N. V.; Vanderkooi, J. M. *J. Mol. Liq.* **2008**, 143, 160.
- (80) Dill, K. A.; Truskett, T. M.; Vlachy, V.; Hribar-Lee, B. *Annu. Rev. Biophys. Biomol. Struct.* **2005**, 34, 173.
- (81) Hribar, B.; Southall, N. T.; Vlachy, V.; Dill, K. A. *J. Am. Chem. Soc.* **2002**, 124, 12302.
- (82) Tielrooij, K. J.; Garcia-Araez, N.; Bonn, M.; Bakker, H. J. *Science* **2010**, 328, 1006.

JP107556S